

Chemical Durability, Structure Properties and Bioactivity of Glasses $48\text{P}_2\text{O}_5\text{-}30\text{CaO}\text{-}(22\text{-}x)\text{Na}_2\text{O}\text{-}x\text{TiO}_2$ (With $0 < x \leq 3$; mol%)

Yassine Er-Rouissi¹, Sara Aqdim², Abdeslam El Bouari², Fouzia Hmimid³, Said Aqdim^{1,4*}

¹Faculty of Sciences, Laboratory of Materials Engineering for Environment and Valorization, Hassan II University Ain Chock, Casablanca, Morocco

²Faculty of Sciences Ben-M'sik, Laboratory Physical-Chemistry of Applied Materials, Hassan II University, Casablanca, Morocco

³Department of Biology, Faculty of Science, Laboratory Health & Environment, Hassan II University Ain Chock, Casablanca, Morocco

⁴Department of Chemistry, Faculty of Science, Mineral Chemistry Laboratory, Hassan II University Ain Chock, Casablanca, Morocco

Email: *said_aq@yahoo.fr

How to cite this paper: Er-Rouissi, Y., Aqdim, S., Bouari, A.E., Hmimid, F. and Aqdim, S. (2020) Chemical Durability, Structure Properties and Bioactivity of Glasses $48\text{P}_2\text{O}_5\text{-}30\text{CaO}\text{-}(22\text{-}x)\text{Na}_2\text{O}\text{-}x\text{TiO}_2$ (With $0 < x \leq 3$; mol%). *Advances in Materials Physics and Chemistry*, 10, 305-318.
<https://doi.org/10.4236/ampc.2020.1012024>

Received: October 10, 2020

Accepted: December 21, 2020

Published: December 24, 2020

Copyright © 2020 by author(s) and Scientific Research Publishing Inc. This work is licensed under the Creative Commons Attribution International License (CC BY 4.0).

<http://creativecommons.org/licenses/by/4.0/>



Open Access

Abstract

Phosphate glasses of composition $48\text{P}_2\text{O}_5\text{-}30\text{CaO}\text{-}(22\text{-}x)\text{Na}_2\text{O}\text{-}x\text{TiO}_2$ (with $0 < x \leq 3$, mol%) were prepared by direct melting at $1080^\circ\text{C} \pm 20^\circ\text{C}$. The chemical durability of these glasses shows an improvement when the TiO_2 content varies from 0 to 2 mol%. The measurements of differential thermal analysis and density, both, indicate the increase of the glass transition temperature and the density. The increase of T_g leads to an improvement of glass rigidity. X-ray diffraction analysis of the glasses annealed at 650°C for 48 h, indicates the appearance of a mixture of metaphosphate and pyrophosphate phases when the TiO_2 content varies from 0 to 2 mol%, the last become majority when the TiO_2 content rich 2 mol%. Nevertheless, when the TiO_2 content exceeds 2 mol%, the analysis, both, by infrared spectroscopy and X-ray diffraction, reveals a radical change of structure with the formation of majorities isolated orthophosphate groups. SEM micrographs illustrated that the number of crystallites increased in the glass network when the TiO_2 content increased at the expense of the Na_2O content. An increase in the TiO_2 content beyond 2 mol% led to the formation of a larger number of crystallites of different sizes, dominated by small crystallite sizes assigned to majority isolated short orthophosphate groups. This phenomenon led to a decrease in chemical durability and seems to be the main cause promoting the bioactivity of glasses. The results of the bioactivity, after a test in an SBF physiological solution within 15 days, shows, both, the formation of hydroxyapatite and trical-

cium phosphate layers, in addition to the layer $\text{Ca}_2\text{P}_2\text{O}_7$, known by its bioactivity, in some samples. The results obtained on the glasses studied make them potential candidates for an application in tissue engineering.

Keywords

Chemical Durability, Phosphate Glasses, Titan Oxide, Bioactivity, SBF

1. Introduction

Several studies have been carried out on phosphate-based glasses as promising materials for various applications in all fields. The properties of phosphate glasses such as low melting point, high thermal expansion coefficient, sealing materials and bioactivity, including the concept of the biomaterials degradation, make them potential candidates for many technological applications [1]-[11]. The bioactivity of phosphate glasses and in particular the property of being completely dissolved in aqueous medium; this degradation concept can be controlled by modifying the intermediate oxides so that the latter are in congruence with the chemical durability and can be used for glasses rich in phosphate and calcium applied as biomaterials [11]-[17]. Calcium phosphate glasses and glass ceramics in the orthophosphate region ($\text{CaO}/\text{P}_2\text{O}_5 = 0.5 - 2$) [18] were obtained by using of other oxides such as Na_2O , Al_2O_3 , Fe_2O_3 , ZnO , MgO , TiO_2 , which can easily depolymerize P_2O_5 oxide from long ultraphosphate ($\text{O}/\text{P} = 2.5$) chains to isolated short orthophosphate chains ($\text{O}/\text{P} = 4$). Our goal is to develop bioactive glasses, focusing particularly on the effect of the substitution of TiO_2 to calcium phosphate oxide glasses for use in the medical field. The study of composition glasses $48\text{P}_2\text{O}_5\text{-}30\text{CaO}\text{-}(22\text{-}x)\text{Na}_2\text{O}\text{-}x\text{TiO}_2$ (with $0 < x \leq 3$; mol%) as a function of the TiO_2 content has shown a rigidity of the glass network in congruence with its biodegradability. The increase in the TiO_2 content (with $0 < x \leq 2$; mol%) in the glass network entrained an increase of the chemical durability, and T_g , followed by an important change from metaphosphate (Q^2) to pyrophosphate structural units (Q^1). When the TiO_2 content beyond 2 mol%, the chemical durability undergo a slow decrease and the structure evolve toward majority isolated short orthophosphate units (Q^0), confirmed by IR spectrum and X-Ray diffraction, SEM micrographs illustrated that the number of crystallites increased in the glass network when the TiO_2 content increased at the expense of the Na_2O content. This indicates that we are near the border between the glass and the crystal [15] [19] [20]. The chemical reactivity of these materials was evaluated after immersion in the simulated body fluid (SBF) at 37°C for 15 days. The analysis results seem important for the beginning of the glasses bioactivity.

2. Experimental Section

Phosphate glasses are prepared by direct melting of the $(\text{NH}_4)\text{H}_2\text{PO}_4$, CaCO_3 ,

Na₂O, TiO₂ mixture in suitable proportions. The reagents are intimately crushed then introduced into a porcelain crucible. Then, they are heated initially at 300°C for 2 h and then at 500°C for 1h to complete the decomposition. The reaction mixture is then heated at 900°C. For 40 minutes and finally at 1080°C. For 30 minutes in order to obtain a homogeneous liquid. Then it is cast in an aluminum plate previously heated to 200°C to avoid thermal shock. Pellets 5 to 10 mm in diameter and 1 to 3 mm thick are obtained. The samples were then immersed in distilled water at 90°C for 20 days to determine the dissolution rate evaluated from the mass loss as a function of time. Analysis by IR spectroscopy was done in a frequency range of between 400 and 1600 cm⁻¹ with a resolution of 2 cm⁻¹, using a Fourier transform spectrometer. The vitreous state was first evidenced from the shiny and transparency aspect, which was then confirmed by X-ray diffraction (XRD) patterns. Samples glasses were analyzed by X-ray diffraction after an annealing time of 48 h at 650°C. Differential thermal analysis (DTA) was performed using a Perkin-Elmer DTA7, at a heating rate of 10°C/min in a flowing nitrogen atmosphere (30 cm³/mn) with alumina crucibles. The Archimedes method was used to measure the density of glasses using orthophthalate as a floating medium. The microstructures of the sample glasses were characterised by scanning electron microscopy (SEM), equipped with a full system micro-analyser (EDX-EDAX). Glass powder of each sample was soaked in SBF solution at 37°C for 21 days.

3. Results and Discussion

3.1. Chemical Durability

The glass series 48P₂O₅-30CaO-(22-x)Na₂O-xTiO₂ (with 0 < x ≤ 3 mol%), was approximated by measuring the dissolution rate (DR) which was defined as the weight loss of the glass expressed in terms g·cm⁻²·mn⁻¹. The DR values reported in **Table 1** show a dissolution decrease versus TiO₂ contents between 0.5 and 2 mole %, after their immersion in 100 ml of distilled water, heated at 90°C for 21 consecutive days (**Figure 1**). However, when the TiO₂ content exceeds 2 mol%, there is a relatively significant increase in the dissolution rate. The value

Table 1. The composition and some characteristics of the quaternary glasses 48P₂O₅-30CaO-(22-x)Na₂O-xTiO₂ (with 0 < x ≤ 3; mol%).

Glass Sample	Starting Oxide mixtures mol %				[O/P] Ratio	log (D _R) (g·cm ⁻² ·min ⁻¹) (±0.2)	T _g (°C) (±2)	T _c (°C) (±2)
	P ₂ O ₅	CaO	Na ₂ O	TiO ₂				
48T05	48	30	21.5	0.5	3046	-4.9	405	495
48T10	48	30	21	1	3052	-5.1	449	498
48T15	48	30	20.5	1.5	3057	-5.7	473	525
48T20	48	30	20	2	3062	-6.05	476	540
48T25	48	30	19.5	2.5	3067	-5.9	430	490
48T30	48	30	19	3	3072	-5.5	450	496

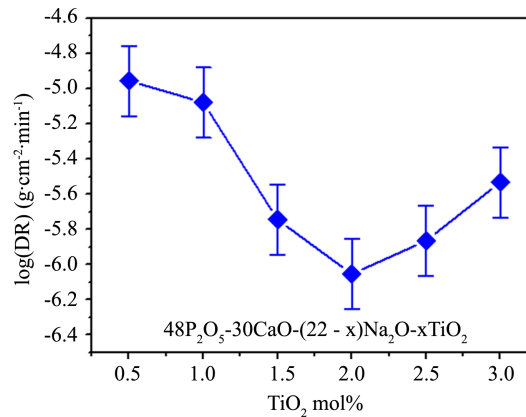


Figure 1. Curve representing the dependency of the chemical durability of the phosphate glasses on the TiO₂ (mol%) level.

of leached pH, for different samples, after 21 days, is represented as a function of the TiO₂ content (**Figure 2**), it indicates that the pH of the solution varies in a range between 3 and 7 ± 0.5, values which correspond to the leached pH of a bioactive glass [18] [21] [22] [23].

3.2. Density and Molar Volumes

The Archimedes principle was used to measure the density of glasses using orthophthalate as a floating medium. The density of the glasses was obtained by using the relation (1),

$$\rho = \left[\frac{m_{\text{air}}}{m_{\text{air}} + m_{\text{ortho}} - m_{(\text{ortho}+\text{glass})}} \right] \rho_{\text{ortho}} \quad (1)$$

With: m_{air} : the mass of the sample measured in the area.

m_{ortho} : Orthophthalate mass only.

$m_{(\text{ortho}+\text{glass})}$: Mass of glass immersed in diethyl orthophthalate.

ρ_{ortho} : 1.11422 g·cm⁻³.

The density variation of composition glasses are represented in **Figure 2**. The molar volume and the anionic radius of the oxygen in the glass were determined respectively from the relationships (2) and (3):

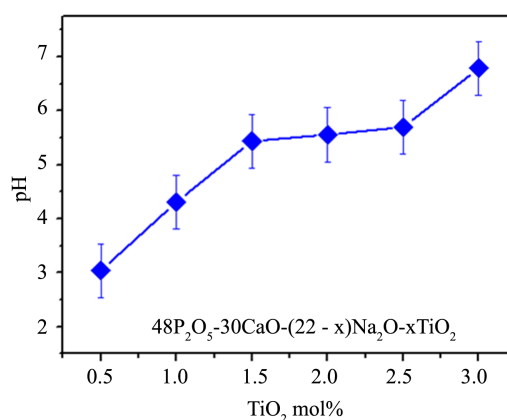
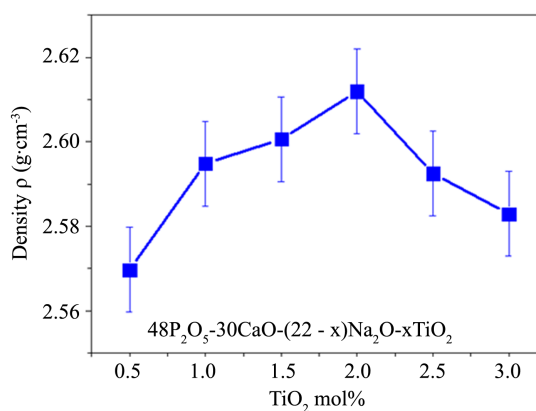
$$V_{0M} = M / \rho N_A N_0^* \quad (2)$$

$$r_{\text{cal}}(\text{O}^{2-}) = 3\sqrt{V_{0M}} / 2 \quad (3)$$

With M = molar mass, ρ = density, N_A = Avogadro number; N_0^* number of oxygen atoms in the molecular formula. The value of the molar volume and the oxygen radius were calculated from the approximate hypothesis of close packing of oxygen anions O²⁻, having $r(\text{O}^{2-})$ recapitulated for each composition in **Table 2** [1] [15]. As can be seen from **Figure 3**, density increased with TiO₂ content at the expense of Na₂O. This seems obvious since the molar mass of titanium oxide is greater than that of sodium oxide. However, when the TiO₂ content becomes greater than 2 mol%, a decrease in the density is noted [9] [13] [14].

Table 2. Glass composition expressed in terms of quaternary system.

Glass sample Code	Chemical compositions (mol%)	Glass compositions inside the ternary diagram
48T05	48P ₂ O ₅ -30CaO-21.5Na ₂ O-0.5TiO ₂	0.3173(Na ₂ O-P ₂ O ₅)-0.0096(TiO ₂ -P ₂ O ₅)-0.6731(CaO-P ₂ O ₅)
48T10	48P ₂ O ₅ -30CaO-21Na ₂ O-1TiO ₂	0.3077 (Na ₂ O-P ₂ O ₅)-0.0192(TiO ₂ -P ₂ O ₅)-0.6731(CaO-P ₂ O ₅)
48T15	48P ₂ O ₅ -30CaO-20.5Na ₂ O-1.5TiO ₂	0.2982(Na ₂ O-P ₂ O ₅)-0.02887(TiO ₂ -P ₂ O ₅)-0.6731(CaO-P ₂ O ₅)
48T20	48P ₂ O ₅ -30CaO-20Na ₂ O-2TiO ₂	0.2884(Na ₂ O-P ₂ O ₅)-0.0385(TiO ₂ -P ₂ O ₅)-0.6731(CaO-P ₂ O ₅)
48T25	48P ₂ O ₅ -30CaO-19.5Na ₂ O-2.5TiO ₂	0.2788(Na ₂ O-P ₂ O ₅)-0.0481(TiO ₂ -P ₂ O ₅)-0.6731(CaO-P ₂ O ₅)
48T30	48P ₂ O ₅ -30CaO-19Na ₂ O-3TiO ₂	0.26923(Na ₂ O-P ₂ O ₅)-0.0576(TiO ₂ -P ₂ O ₅)-0.6731(CaO-P ₂ O ₅)

**Figure 2.** evolution of the lixiviate pH versus of TiO₂ content for 21 days of attack in distilled water at 90°C.**Figure 3.** Variation of the Density (ρ) versus TiO₂ mol% along the Glass series 48P₂O₅-30CaO-(22-x)Na₂O-xTiO₂.

3.3. Infra-Red Spectra

The infrared spectra of 48P₂O₅-30CaO-(22-x)Na₂O-xTiO₂ series glasses (with 0 < x ≤ 3) are shown in **Figure 4**. All the vibration bands of the treated samples are in the frequency range from 1400 to 400 cm⁻¹. Analysis of the infrared spectra obtained for all the glasses shows a wide band at around 510 cm⁻¹ attributed to the vibration mode of the skeleton δ (P-O-P) [1] [3] [9]. The vibration bands located around 754 - 784 cm⁻¹ are attributed to the vibration mode ν_{sym} (P-O-P)

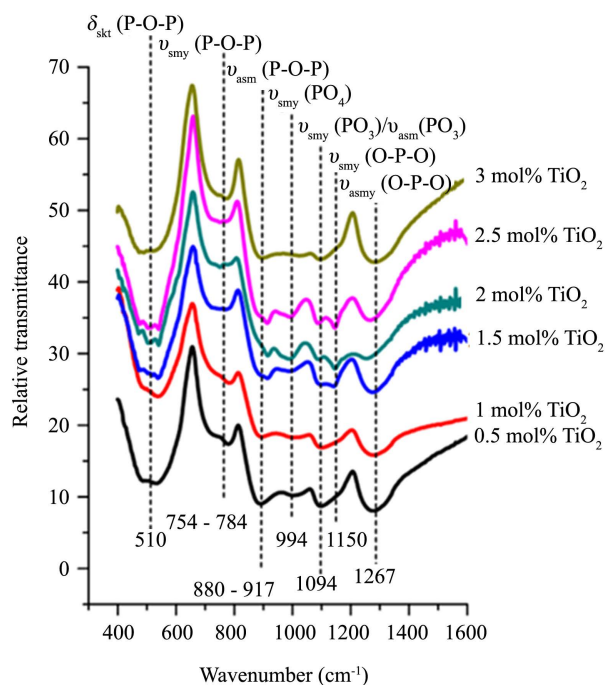
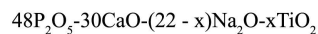
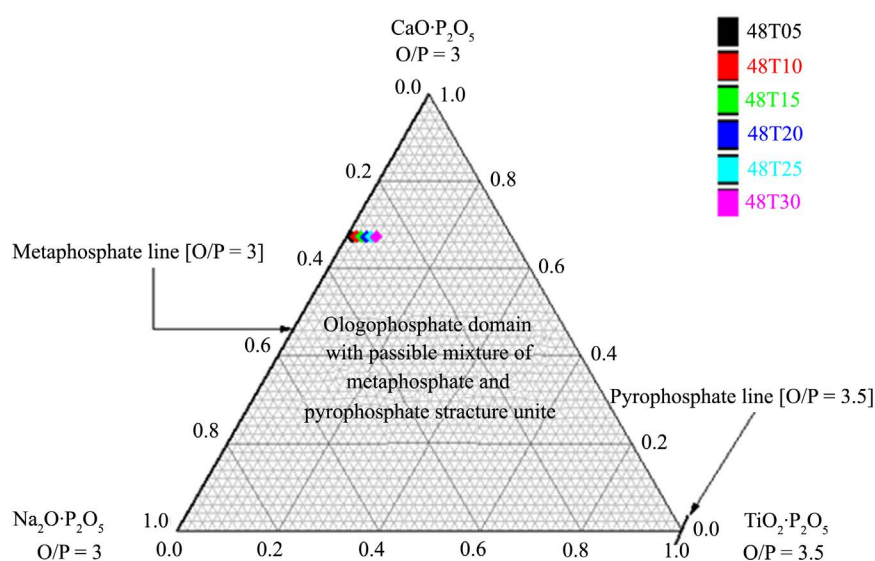


Figure 4. IR spectra of phosphate glasses of composition $48\text{P}_2\text{O}_5\text{-}30\text{CaO}\text{-}(22-x)\text{Na}_2\text{O}\text{-}x\text{TiO}_2$.

of pyrophosphate groups (Q^1), while the bands at around 1094 cm^{-1} and 1267 cm^{-1} are respectively assigned to the $\text{V}_{\text{sym}}(\text{PO}_2)/\text{V}_{\text{asy}}(\text{PO}_3)$ of pyrophosphate groups (Q^1) and vibration mode $\text{V}_{\text{asy}}(\text{PO}_2)$ of metaphosphate groups (Q^2) [2] [4] [5] [9] [12]. The band at around 1150 cm^{-1} , attributed to the stretching vibration $\text{V}_{\text{sym}}(\text{PO}_2)$ in $\text{Q}^1 - \text{Q}^2$ units, appears when the TiO_2 content increased in the glass network [4] [9] [12], while the intensity of the band 1267 cm^{-1} attributed to metaphosphates groups (Q^2) decreased. In the other hand, the band at $880 - 917\text{ cm}^{-1}$, attributed to asymmetric vibration $\text{V}_{\text{asy}}(\text{P-O-P})$ in the Q^1 unit, shift to high frequencies as the TiO_2 content increased in the network glass [2] [4] [5] [9] [15]. However, the characteristic vibration band of $\text{V}_{\text{sym}}(\text{PO}_4^{3-})$ in the Q^0 unit, located around 994 cm^{-1} , appeared when the TiO_2 content becomes greater than 1.5 mol%, while the band at 1094 cm^{-1} , attributed to the $\text{V}_{\text{sym}}(\text{PO}_2)/\text{V}_{\text{asy}}(\text{PO}_3)$ vibration mode of pyrophosphate groups, becomes smaller and smaller [9] [24]. Furthermore, the structure deduced from vibrational spectroscopy is compatible with the localization analysis of the compounds (45T05, 45T10, 45T15) inside the ternary diagram given in **Figure 5** and **Table 3**. However, when the TiO_2 content increased beyond 1.5 mole% (45T20, 45T25), we noticed the appearance, in addition to the oligophosphate groups ($\text{Q}^1 - \text{Q}^2$), of isolated short ortho phosphate groups (Q°) [16] [25] which indicated the approach of the border area between glass and crystal, this can be explained by several factors (high T_f of TiO_2 , crystallite level in the glass bath, $\text{Ti} + \text{Ca}/\text{P}$ ratio) [15] [20].

Table 3. Density and related molar data of the $48\text{P}_2\text{O}_5\text{-}30\text{CaO}\text{-}(22\text{-}x)\text{Na}_2\text{O}\text{-}x\text{TiO}_2$ system.

Glass sample code	Starting oxide mixtures mol %				ρ ($\text{g}\cdot\text{cm}^{-3}$) (± 0.01)	Molar mass ($\text{g}\cdot\text{mol}^{-1}$)	Molar volume (\AA^3) $V_{oM} = M/[\rho N_A N_o^*]$	Calculated oxygen radius (\AA) $r_{\text{cal}} (\text{O}^{2-})$
	P_2O_5	CaO	Na_2O	TiO_2				
48T05	48	30	21.5	0.5	2.57	98,719	21.81	1397
48T10	48	30	21	1	2.59	98,809	21.58	1392
48T15	48	30	20.5	1.5	2.60	98,898	21.52	1390
48T20	48	30	20	2	2.61	98,988	21.40	1388
48T25	48	30	19.5	2.5	2.59	990,775	21.55	1391
48T30	48	30	19	3	2.58	101,564	22.13	1403

**Figure 5.** Localization of the investigate glass compositions 48T05 \rightarrow 48T25 within the ternary diagram $(\text{CaO}\cdot\text{P}_2\text{O}_5)\text{-}(\text{Na}_2\text{O}\cdot\text{P}_2\text{O}_5)\text{-}(\text{TiO}_2\cdot\text{P}_2\text{O}_5)$. The table gives the corresponding compositions within the quaternary system $(\text{P}_2\text{O}_5\text{-}\text{CaO}\text{-}\text{Na}_2\text{O}\text{-}\text{TiO}_2)$.

3.4. X-Ray Diffraction and DTA

As expected, X-ray crystallography confirmed the vitreous nature of all the investigated glass samples studied. In fact, X-ray diffraction pattern (XRD) recordings show the absence of diffraction peaks. DSC of the glasses (**Figure 6**) indicates both an increase in the glass transition temperature and the crystallization temperature versus Ti_2O content. When the Ti_2O content increases from 0.5 to 2 mol%, the glass transition temperature (T_g) increases in the 405°C - 476°C range, whereas the crystallization temperature (T_c) increases in the 495°C - 540°C range (see **Table 1**) [24]. Beyond 2 mole %, the glass transition temperature (T_g) and the crystallisation temperature T_c undergo, respectively, a decrease from 476°C to 430°C and from 540°C to 490°C . The heat treatment of the 48T15, 48T20 and 48T25 glasses at 650, gives the XRD patterns shown in **Figure 7**. These spectra show a structural evolution from metaphosphate to pyrophosphate

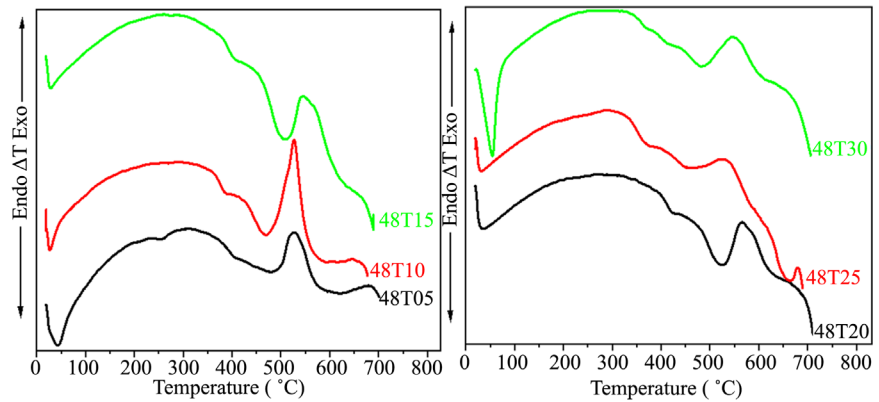


Figure 6. Differential thermal analysis (DTA) of glass compositions $48P_2O_5-30CaO-(22-x)Na_2O-xTiO_2$.

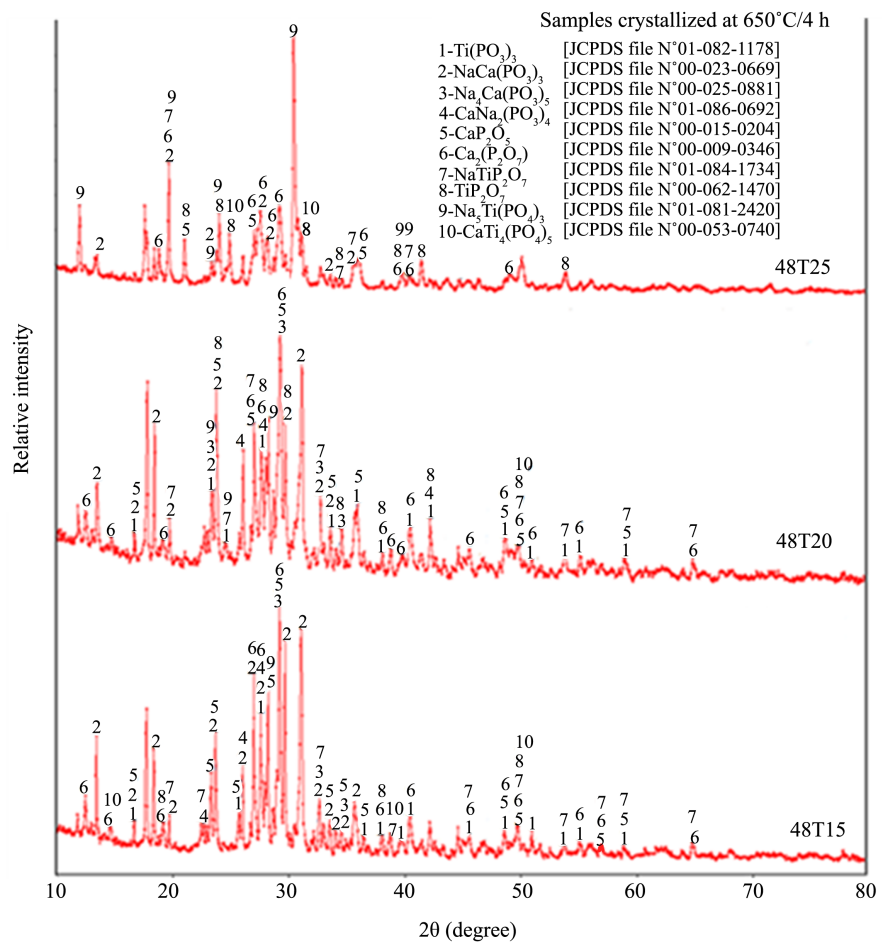


Figure 7. XRD patterns for glass samples 48T05, 48T15 and 48T25 after heat treatment for 48 hrs under air atmosphere at 650°C.

and finally to orthophosphates phases. When the 48T15 sample was thermally treated at 650°C, the amorphous phase partially disappeared and majority Ti(PO₃)₃ [JCPDS files N°: 01-082-1178], NaCa(PO₃)₃ [JCPDS files N°: 00-23-0669], Na₂Ca(PO₃)₆, [JCPDS files N°: 00-025-0811] and **CaP₂O₆** [JCPDS files N°:

00-015-0204] (cyclic metaphosphate O/P = 3), with minor $\text{Ca}_2\text{P}_2\text{O}_7$ [JCDDS files N°: 00-009-0346] and $\text{Na}_5\text{Ti}_4(\text{PO}_4)_6$ [JCPDS files N°: 01-081-2420] phases occurred in the sample. When the TiO_2 content increased in the glass (48T20), the heat treatment at 650°C caused the formation of NaTiP_2O_7 [JCPDS file N°: 01-084-1137-], $\text{Ca}_2\text{P}_2\text{O}_7$ [JCPDS file N°: 00-009-0346] and TiP_2O_7 [JCPDS file N°00-052-1470] with some trace of metaphosphate and isolated short orthophosphates phases, and indicated the increase of pyrophosphate phases (O/P = 3.5). However, when the TiO_2 content exceeded 2 mol% (48T25), the heat treatment, at the same temperature, indicated the majority formation of $\text{Na}_5\text{Ti}(\text{PO}_4)_3$ [JCPDS file N°: 01-081-2421] and $\text{CaTi}_4(\text{PO}_4)_6$ [JCPDS file N°: 00-053-0740] phases to the detriment of the pyrophosphates and metaphosphate phases [23] [25] [26].

3.5. SEM Image Analysed

The SEM micrograph shows the existence of two phases, one crystalline and the other glassy (**Figure 8**). It also indicates the formation of crystalline phase agglomerates of different sizes [2] [15] [21] [24] [25]. Thus, a structural change is observed from **Figure 8(a)** to **Figure 8(b)** which presumably indicates the

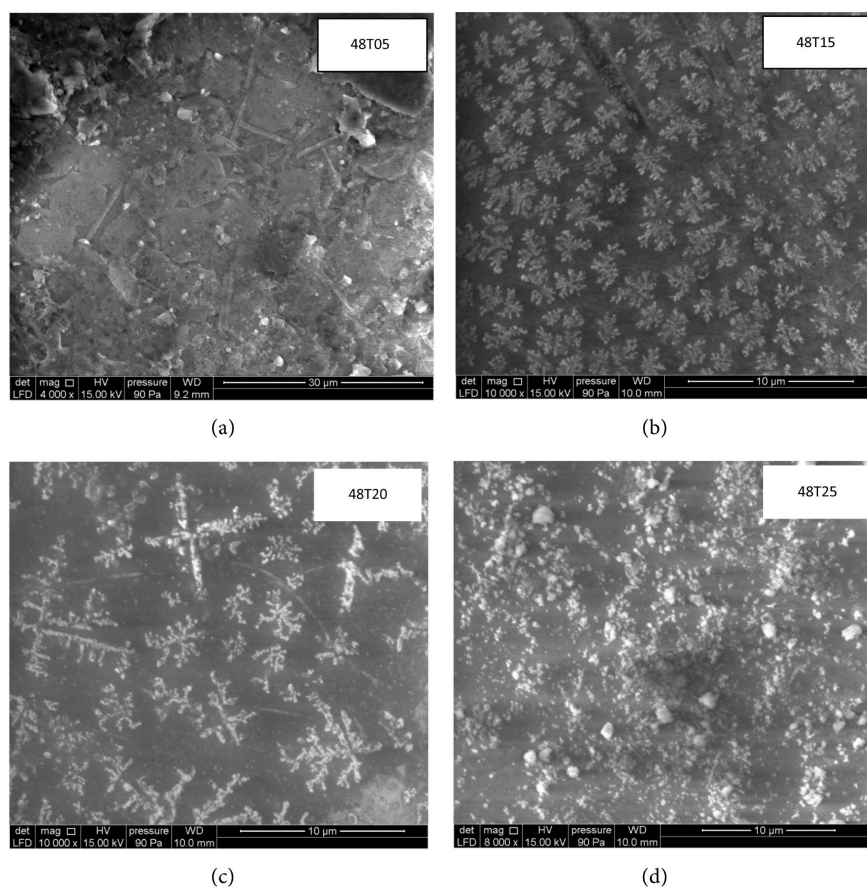


Figure 8. SEM optical micrograph showing the structural evolution of phosphate glasses from 48T05 to 48T20.

formation of the predominant cyclic metaphosphate phases. However, when looking at **Figure 8(c)** there is a structural mixture between cyclic metaphosphates and, presumably, of short pyrophosphate chains. In **Figure 8(d)**, there is a radical change in the structure from the pyrophosphate groups towards predominantly isolated shorter orthophosphate groups. Consequently, the increase of TiO_2 content in the glassy network leads to a progressive depolymerization of the cyclic metaphosphate groups towards pyrophosphate groups and finally to isolated short orthophosphate groups [24] [25].

3.6. *In Vitro* Bioactivity of Studies Glasses-Surface Analysis Using X-Ray Diffraction

The study *in vitro* bioactivity of the prepared glasses was carried out by analyzing X-ray diffraction spectra of the samples after immersion in the simulated body fluid (SBF) for 15 days at 37°C . The result showed (**Figure 9**) that for the majority of studied glasses there is formation, both, of hydroxyapatite and tricalcium phosphate layers on the surfaces of the samples in addition to the $\text{Ca}_2\text{P}_2\text{O}_7$ phase known by its bioactivity [16]. When the TiO_2 content increases in the glass, the HA and tricalcium phosphate phases become more evident. The number of peaks and their intensities increase, while the peak intensity of the CaP_2O_7 phase decreases. The peaks of tricalcium phosphate appear at 22.84 and 24.10 (2θ) are assigned, respectively, to (241) and (132) reflections [JCPDS file N°00-033-0297], However the peaks of HA located at 26.40, 28 and 32.83 (2θ) assign respectively to (002), (102) and (300) reflections [JCPDS file N°01-074-0566] [27]. The peaks of $\text{Ca}_2\text{P}_2\text{O}_7$ phase appear at 30 and 31.92 (2θ) are assigned respectively to (211) and (123) reflections [JCPDS file N°00-033-0297].

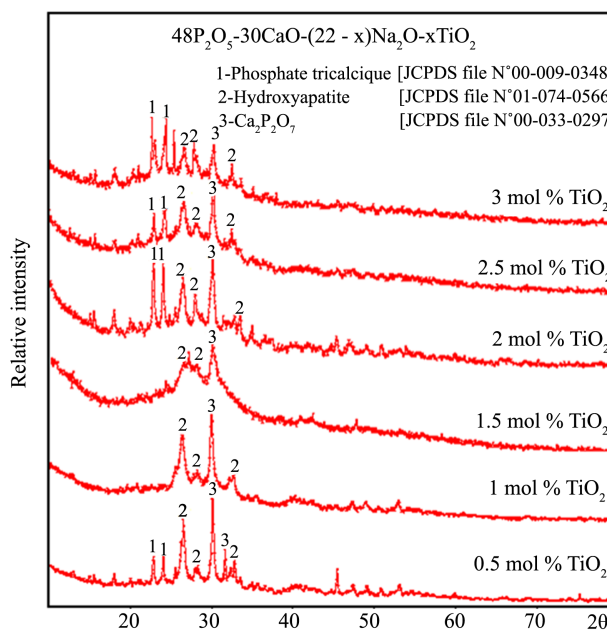


Figure 9. XRD patterns for the surface of the phosphate glasses doped with titanium 48T05 \rightarrow 48T30, after 15 days of immersion in SBF.

A deep analysis of the spectra obtained seems to suggest that the tricalcium phosphate layer is more important than the hydroxyapatite phase when the TiO_2 content reaches 3 mol%.

4. Discussion

Phosphate glasses of composition $48\text{P}_2\text{O}_5\text{-}30\text{CaO}\text{-}(22\text{-}x)\text{Na}_2\text{O}\text{-}x\text{TiO}_2$ (with $0 < x \leq 3$; mol%) have been investigated. The structure and the chemical durability have been studied using various techniques such as IR, XRD, DSC, SEM... Both X-ray diffraction and IR spectroscopy have confirmed the structure change from metaphosphate to oligophosphates when the TiO_2 content increases from 0.5 to 2 mol% in the glass. However, beyond 2 mol% of TiO_2 , the appearance of isolated orthophosphate groups is observed. The scanning electron microscope indicated a morphological change from one cliche to another as the TiO_2 content increased from 0.5 to 2.5 mol%. This change elucidates the passage from cyclic metaphosphate groups to oligophosphate (mixture meta and pyrophosphate) and finally to isolated short ortho phosphate groups. The variation of transition temperature versus TiO_2 content indicated an increase in T_g from 405°C to 430°C when the TiO_2 content increased from 0.5 to 2 mol%, elucidating an improvement in the rigidity of the glass [26] [28]. Beyond 2 mol% TiO_2 , the transition temperature (T_g) decreased from 430°C to 395°C , indicating a slight weakness of the glass due to the radical change of structure by the formation, of isolated ortho phosphate groups, confirmed, both, by IR spectroscopy and XRD [12] [15] [20]. The increase of isolated short orthophosphate chains in the glass network, at the expense of oligophosphate chains, when the Ti_2O content exceeded 2 mol%, can be explained by the fact that we were close to the border area between crystal and glass [15] [20]. The number of crystallites of different sizes generally increased and exceeded the equilibrium that must be established between the glass bath and the crystallites; hence, we note a significant decrease in chemical durability. At the light of the results obtained, both, for chemical durability, X-ray diffraction and IR spectra analysis ($D_R \approx 10^{-6} \text{ g}\cdot\text{cm}^{-2}\cdot\text{min}^{-1}$, development of isolated orthophosphate groups (PO_4^{3-}) [20] [23], the chemical reactivity of these materials studied was evaluated after immersion in the simulated body fluid (SBF) at 37°C for 15 days. Once in contact with the biological fluids (SBF solution), the bioactive glasses presented the particularity of generating a series of physicochemical reaction to the liquid-glass interface [17] [18] [20]. This series of reactions constitutes the mechanism of bioactivity. The XRD spectra, after test *in vitro*, indicate the formation of a mixture of hydroxyapatite and tricalcium layers in addition of some traces of calcium pyrophosphate phases, known for its bioactivity [25]. An in-depth analysis of the X-ray spectra obtained, after immersion in the simulated body fluid (SBF), showed that, both, the formation of tricalcium phosphate and of hydroxyapatite layers become more important when the TiO_2 content reached 3 mol%, which, further elucidates that the bioactivity of glasses is like to be greatly successful when once the glass composition is close to the border zone between glass and

crystal. In addition, bioactivity appeared in all glasses studied, even those which contain traces of isolated short orthophosphate groups ($x \leq 2$ mol%), this, probably, proves that these last ones are the triggers of bioactivity in the glasses.

5. Conclusion

The influence of TiO_2 on the glass forming characteristics and properties of $\text{Na}_2\text{O-TiO}_2\text{-CaO-P}_2\text{O}_5$ glasses has been investigated. The structure and the chemical durability have been studied using various techniques such IR, XRD, DSC, SEM. The variation of the transition temperature versus TiO_2 content indicates an increase in T_g when the TiO_2 content increases and indicates an improvement in the rigidity of the glass. SEM micrograph indicates the existence of two phases one crystalline and the other vitreous. The morphological of the phase crystalline change from one micrograph to another as the TiO_2 content increases from 0.5 to 2.5 mol% and indicates that the structure moves from cyclic metaphosphate and oligophosphate groups to orthophosphate groups. The chemical reactivity of these materials was evaluated after contacting the different glasses with a synthetic physiological fluid (SBF). The XRD spectra of these glasses, after test *in vitro*, indicate the formation of a mixture of hydroxyapatite and tricalcium layers with some traces of calcium pyrophosphate phases. The presence of these layers is very interested for an eventual biological application *in vivo*.

Acknowledgements

The authors wish to thank National Center for Scientific and Technical Research [Division of Technical Support Unit for Scientific Research (TSUSR) Rabat, Morocco] for their assistance to the realization of this work. We also thank Ms. Pr. R. ELOUATIB (Laboratory physic and chemistry of inorganic materials) for the support that has brought us.

Conflicts of Interest

The authors declare no conflicts of interest regarding the publication of this paper.

References

- [1] Aqdim, S., Sayouty, E.H., Elouadi, B. and Greneche, J.M. (2012) Chemical Durability and Structural Approach of the Glass Series $(40-y) \text{Na}_2\text{O-yFe}_2\text{O}_3\text{-5Al}_2\text{O}_3\text{-55P}_2\text{O}_5$ -by IR, X-Ray Diffraction and Mössbauer Spectroscopy. *IOP Conference Series: Materials Science and Engineering*, **28**, 012003. <https://doi.org/10.1088/1757-899X/28/1/012003>
- [2] Aqdim, S. and Ouchetto, M. (2013) Elaboration and Structural Investigation of Iron (III) Phosphate Glasses. *Advances in Materials Physics and Chemistry*, **3**, 332-339. <http://dx.doi.org/10.4236/ampc.2013.38046>
- [3] Lai, Y.M., Liang, X.F., Yang, S.Y., Wang, J.X. and Zhang, B.T. (2012) Raman Spectra Study of Iron Phosphate Glasses with Sodium Sulfate. *Journal of Molecular Struc-*

- ture, **1013**, 134-137. <https://doi.org/10.1016/j.molstruc.2012.01.025>
- [4] Morikawa, H., Lee, S., Kasuga, T. and Brauer, D.S. (2013) Effects of for Calcium Substitution in P_2O_5 -CaO-TiO₂ Glasses. *Journal of Non-Crystalline Solids*, **380**, 53-59. <https://doi.org/10.1016/j.jnoncrysol.2013.08.029>
- [5] Chabbou, Z. and Aqdim, S. (2014) Chemical Durability and Structural Proprieties of the Vitreous Part of the System $x\text{CaO}-(40-x)\text{ZnO}-15\text{Na}_2\text{O}-45\text{P}_2\text{O}_5$. *Advances in Materials Physics and Chemistry*, **4**, 179-186. <http://dx.doi.org/10.4236/ampc.2014.410021>
- [6] Bengisu, M., Brow, R.K., Yilmaz, E., Moguš-Milanković, A. and Reis, S.T. (2006) Aluminoborate and Aluminoborosilicate Glasses with High Chemical Durability and the Effect of P_2O_5 Additions on the Properties. *Journal of Non-Crystalline Solids*, **352**, 3668-3676. <https://doi.org/10.1016/j.jnoncrysol.2006.02.118>
- [7] Day, D.E., Wu, Z., Ray, C.S. and Hrma, P. (1998) Chemically Durable Iron Phosphate Glass Wasteforms. *Journal of Non-Crystalline Solids*, **241**, 1-12. [https://doi.org/10.1016/S0022-3093\(98\)00759-5](https://doi.org/10.1016/S0022-3093(98)00759-5)
- [8] Bingham, P.A. and Hand, R.J. (2005) Vitriified Metal Finishing Wastes: I. Composition, Density and Chemical Durability. *Journal of Hazardous Materials*, **119**, 125-133. <https://doi.org/10.1016/j.jhazmat.2004.11.014>
- [9] Shaim, A. and Et-Tabirou, M. (2003) Role of Titanium in Sodium Titanophosphate Glasses and a Model of Structural Units. *Materials Chemistry and Physics*, **80**, 63-67. [https://doi.org/10.1016/S0254-0584\(02\)00087-1](https://doi.org/10.1016/S0254-0584(02)00087-1)
- [10] McLaughlin, J.C., Tagg, S.L., Zwanziger, J.W., Haeffner, D.R. and Shastri, S.D. (2000) The Structure of Tellurite Glass: A Combined NMR, Neutron Diffraction, and X-Ray Diffraction Study. *Journal of Non-Crystalline Solids*, **274**, 1-8. [https://doi.org/10.1016/S0022-3093\(00\)00199-X](https://doi.org/10.1016/S0022-3093(00)00199-X)
- [11] Weiss, D.S.L., Torres, R.D., Buchner, S., Blunk, S. and Soares, P. (2014) Effect of Ti and Mg Dopants on the Mechanical Properties, Solubility, and Bioactivity *in Vitro* of a Sr-Containing Phosphate Based Glass. *Journal of Non-Crystalline Solids*, **386**, 34-38. <https://doi.org/10.1016/j.jnoncrysol.2013.11.036>
- [12] Brow, R.K., Click, C.A. and Alam, T.M. (2000) Modifier Coordination and Phosphate Glass Networks. *Journal of Non-Crystalline Solids*, **274**, 9-16. [https://doi.org/10.1016/S0022-3093\(00\)00178-2](https://doi.org/10.1016/S0022-3093(00)00178-2)
- [13] Rajendran, V., Devi, A.G., Azooz, M. and El-Batal, F.H. (2007) Physicochemical Studies of Phosphate Based P_2O_5 - Na_2O -CaO-TiO₂ Glasses for Biomedical Applications. *Journal of Non-Crystalline Solids*, **353**, 77-84. <https://doi.org/10.1016/j.jnoncrysol.2006.08.047>
- [14] Kiani, A., Hanna, J.V., King, S.P., Rees, G.J., Smith, M.E., Roohpour, N. and Knowles, J.C. (2012) Structural Characterization and Physical Properties of P_2O_5 -CaO- Na_2O -TiO₂ Glasses by Fourier Transform Infrared, Raman and Solid-State Magic Angle Spinning Nuclear Magnetic Resonance Spectroscopies. *Acta Biomaterial*, **8**, 333-340. <https://doi.org/10.1016/j.actbio.2011.08.025>
- [15] Errouissi, Y., Z. Chabbou, N. Beloued, S. Aqdim and Aqdim, S. (2017) Chemical Durability and Structural Properties of Al_2O_3 -CaO- Na_2O - P_2O_5 Glasses Studied by IR Spectroscopy, XRD and SEM. *Advances in Materials Physics and Chemistry*, **7**, 353-363. <https://doi.org/10.4236/ampc.2017.710028>
- [16] Moss, R.M., Abou Neel, E.A., Pickup, D.M., Twyman, H.L., Martin, R.A., Henson, M.D., Barney, E.R., Hannon, A.C., Knowles, J.C. and Newport, R.J. (2010) The Effect of Zinc and Titanium on the Structure of Calcium-Sodium Phosphate Based Glass. *Journal of Non-Crystalline Solids*, **356**, 1319-1324.

- <https://doi.org/10.1016/j.jnoncrysol.2010.03.006>
- [17] Pardini, A. (2007) Laboration et Analyses Structurales de Bioactifs Macroporeux. These de Doctorat, Université de Valenciennes et du Hainaut Cambrés, Valenciennes.
- [18] Mullier, C. (2011) Synthèse et Caractérisation de biomatériaux phosphocalciques multiphasés dopés ou non avec des inhibiteurs de la Résorption Osseuse, These de Doctorat, Faculté des Sciences & Techniques, Université de Nantes, France.
- [19] Makhoul, R., Beloued, N. and Aqdim, S. (2018) Study of Chromium-Lead-Phosphate Glasses by XRD, IR, Density and Chemical Durability. *Advances in Materials Physics and Chemistry*, **8**, 269-280. <https://doi.org/10.4236/ampc.2018.86018>
- [20] Beloued, N., Chabbou, Z. and Aqdim, S. (2016) Correlation between Chemical Durability Behaviour and Structural Approach of the Vitreous Part of the System $55\text{P}_2\text{O}_5-2\text{Cr}_2\text{O}_3-(43-x)\text{Na}_2\text{O}-x\text{PbO}$. *Advances in Materials Physics and Chemistry*, **6**, 149-156. <http://dx.doi.org/10.4236/ampc.2016.66016>
- [21] Lakhkar, N.J., Park, J.-H., Mordan Vehid Salih, N.J., Wall, I.B., Kim, H.-W., King, S.P., Hanna, J.V., Martin, R.A., Addison, O., Mosselmans, J.F.W. and Knowles, J.C. (2012) Titanium Phosphate Glass Microspheres for Bone Tissue Engineering. *Acta Biomaterialia*, **8**, 4181-4190. <https://doi.org/10.1016/j.actbio.2012.07.023>
- [22] Cédric, B. (2008) Elaboration et Caractérisation d'un Hybride Organominéral à Base de Polycaprolactone et de Bioverre sous Forme de Mousse Macroporeuse Pour la Régénération Osseuse. Thèse d'Université, Spécialité Sciences des Matériaux, Ecole Doctorale des Sciences Fondamentales, France.
- [23] Melba, N., Ginebra, M.-P., Clement, J., Martí'nez, S., Avila, G. and Planell, J.A. (2003) Physicochemical Degradation of Titania-Stabilized Soluble Phosphate Glasses for Medical Applications. *Journal of the American Ceramic Society*, **86**, 1345-1352. <https://doi.org/10.1111/j.1151-2916.2003.tb03474.x>
- [24] Monem, A.S., El Batal, H.A., Khalil, E.M.A., Azooz, M.A. and Hamdy, Y.M. (2008) *In Vivo* Behavior of Bioactive Phosphate Glass-Ceramics from the System $\text{P}_2\text{O}_5-\text{Na}_2\text{O}-\text{CaO}$ Containing TiO_2 . *Journal of Materials Science: Materials in Medicine*, **19**, 1097-1108. <https://doi.org/10.1007/s10856-007-3044-3>
- [25] El Batal, H.A., Khalil, E.M.A. and Hamdy, Y.M. (2008) *In Vitro* Behavior of Bioactive Phosphate Glass-Ceramics From the System $\text{P}_2\text{O}_5-\text{Na}_2\text{O}-\text{CaO}$ Containing Titania. *Ceramics International*, **35**, 1195-1204. <https://doi.org/10.1016/j.ceramint.2008.06.004>
- [26] Ali Abou Neel, E., Chrzanowski, W. and Campbell Knowles, J. (2008) Effect of Increasing Titanium Dioxide Content on Bulk and Surface Properties of Phosphate-Based Glasses. *Acta Biomaterialia*, **4**, 523-534. <https://doi.org/10.1016/j.actbio.2007.11.007>
- [27] Mathew, M., Schroeder, L.W., Dickens, B. and Brown, W.E. (1977) The Crystal Structure of $\alpha\text{-Ca}_3(\text{PO}_4)_2$. *Acta Crystallographica Section B*, **33**, 1325-1333. <https://doi.org/10.1107/S0567740877006037>
- [28] Beloued, N., Makhoul, R., Er-Rouissi, Y., Taibi, M., Sajieddine, M. and Aqdim, S. (2019) Relationship between Chemical Durability, Structure and the Ionic-Covalent Character of Me-O-P Bond (Me=Cr, Fe), in the Vitreous Part of the System $60\text{P}_2\text{O}_5-2\text{Cr}_2\text{O}_3-(38-x)\text{Na}_2\text{O}-x\text{Fe}_2\text{O}_3$ (with $3 \leq x \leq 33$ mol%). *Advances in Materials Physics and Chemistry*, **9**, 199-209.